Research Article

Received: 11 April 2016 Revised: 3 May 2016 Accepted article published: 24 May 2016 Published online in Wiley Online Library: 24 June 2016

(wileyonlinelibrary.com) DOI 10.1002/ps.4323

Phthalimide-derived strigolactone mimics as germinating agents for seeds of parasitic weeds

Antonio Cala,[a] Kala Ghooray,[a] Mónica Fernández-Aparicio,[b] José MG Molinillo,[a] Juan CG Galindo,[a] Diego Rubiales[c] and Francisco A Macías[a]*

Abstract

BACKGROUND: Broomrapes attack important crops, cause severe yield losses and are difficult to eliminate because their seed bank is virtually indestructible. In the absence of a host, the induction of seed germination leads to inevitable death due to nutrient starvation. Synthetic analogues of germination-inducing factors may constitute a cheap and feasible strategy to control the seed bank. These compounds should be easy and cheap to synthesise, as this will allow their mass production. The aim of this work is to obtain new synthethic germinating agents.

RESULTS: Nineteen *N*-substituted phthalimides containing a butenolide ring and different substituents in the aromatic ring were synthesised. The synthesis started with commercially available phthalimides. The complete collection was assayed against the parasitic weeds *Orobanche minor*, *O. cumana*, *Phelipanche ramosa* and *P. aegyptiaca*, with the synthetic strigolactone analogue GR24 used as a positive control. These compounds offered low EC_{50} values: *O. cumana* 38.3 μM, *O. minor* 3.77 μM, *P. aegyptiaca* 1.35 μM and *P. ramosa* 1.49 μM.

CONCLUSIONS: The synthesis was carried out in a few steps and provided the target compounds in good yields. The compounds tested showed great selectivity, and low EC_{50} values were obtained for structures that were simpler than GR24.

Supporting information may be found in the online version of this article.

Keywords: broomrape; seed germination; strigolactone; phthalimide; butenolide; GR24

1 INTRODUCTION

Broomrapes (*Orobanche* and *Phelipanche* species) are obligate holoparasitic plants that attack numerous important crops and cause severe yield losses in the Mediterranean region, Central and Eastern Europe and Asia.[1] Current control strategies have had little effect in preventing crop damage from broomrapes. The main obstacle for broomrape control is their highly persistent parasitic seed bank. This seed bank resilience is due to long-term seed viability, high fecundity and the fact that they only germinate in the presence of host plants.

The broomrape seed bank can lie dormant in superficial soil for many years in the absence of appropriate conditions for seedling establishment. Parasite germination is only triggered in the presence of three signals (temperature, humidity and host growth, which indicates nutrient availability). In order to recognise the presence of a host, broomrape seeds require a period of warm stratification called seed conditioning.[2–4] Seed conditioning in this case involves germination inducers that can activate parasitic seed receptors in the same way that host roots do. Broomrapes germinate when they recognise germination-inducing factors exuded by host roots;[4] thus, molecules that can induce seed germination in the absence of the host plant represent a promising strategy for broomrape control. Several molecules have been identified as having activity as germination-inducing factors for parasitic plants, e.g. strigolactones (*Striga*, *Orobanche*, *Phelipanche*),[5,6] dehydrocostuslactone (*O. cumana*),[7] isothiocyanates (*P. ramosa*),[8] peagol and peagoldione (*O. foetida*, *P. aegyptiaca*),[9] peapolyphenols A to C (*Orobanche*, *Phelipanche*),[10] soyasapogenol B (*O. minor*) and *trans*-22-dehydrocampesterol (*Orobanche*, *Phelipanche*).[11]

In general, weedy species of broomrape have a broader range of hosts than wild species,[12] although differences in the host range do exist between species of broomrape weeds. For example, *P. aegyptiaca* has a wide range of hosts, while others, such as *O. cumana*,[13] display a high degree of specialisation. For successful parasitism to occur, there must be a compatible pair of

* *Correspondence to: FA Macías, Department of Organic Chemistry, School of Science, University of Cádiz, C/República Saharaui, 7, 11510-Puerto Real, Cádiz, Spain. E-mail: famacias@uca.es*

a *Allelopathy Group, Department of Organic Chemistry, Institute of Biomolecules, School of Science, University of Cadiz, Puerto Real, Cádiz, Spain*

b *INRA-UMR, 1347, Agroécologie, Dijon, France*

c *Institute for Sustainable Agriculture, CSIC, Córdoba, Spain*

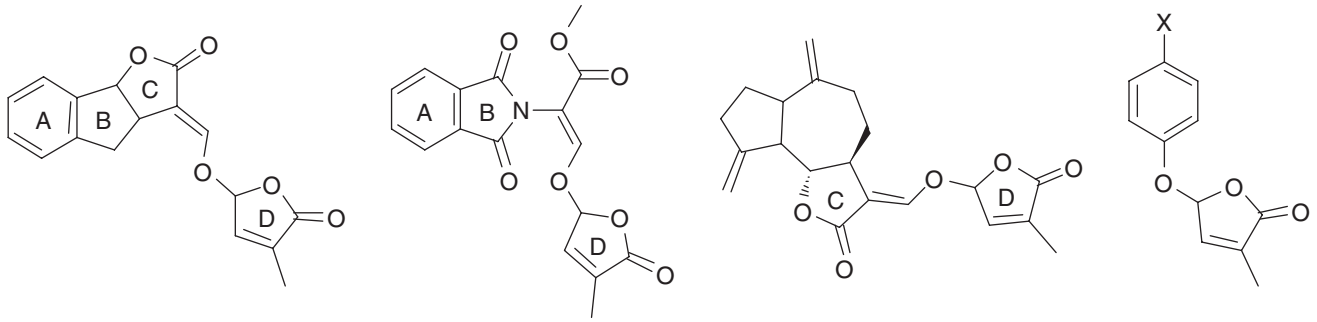

Figure 1. Analogues of strigolactones GR24, Nijmegen-1 and Guaianestrigolactone that stimulate the germination of parasitic weeds (X = Br, I, CF_3, CN).

crop–broomrape species in a given agricultural field. The first level of compatibility in the species-specific parasitic process occurs during germination, which is dependent on both the specific induction potential of host root exudates and the capability of broomrape seeds to recognise those chemical signals.[14,15] As a result of this germination strategy, the seed bank of parasitic weeds synchronises the onset of their life cycle with the cultivation of susceptible crops. In the absence of such crops, the seeds remain dormant and are viable for up to two decades, which precludes the cultivation of susceptible hosts in that particular area for prolonged periods.[16]

In the absence of hosts, broomrape seed germination is considered suicidal because the broomrape seedling is unable to survive longer than a few days in the absence of a host-derived nutrient supply. Suicidal germination is an important strategy for broomrape seed bank control,[17] and it has proven to be successful for the almost complete eradication of *Striga* weed in the United States.[1,18] In the last year, the technical feasibility of suicidal germination was proven for the treatment of sorghum infested with *Striga hermonthica*. Soil application of formulated T-010 reduced *Striga* emergence by 33% and increased sorghum growth.[19]

Exogenous applications of hormones such as ethylene, cytokinin (CK) and gibberellins (GA) have proven to be active in promoting the germination of dormant seeds in many non-parasitic species. However, such treatment does not induce broomrape germination in the absence of strigolactones.[20–24]

N-Substituted phthalimides elicit GA-like germination activity in dormant seeds of several species.[25–27] Recent findings by McCourt *et al.*[24,28] on cotylimides suggest that these structurally unrelated molecules to strigolactones may open up new alternatives to strigolactone analogues.

N-Substituted phthalimides might also constitute a cheap alternative to natural bioregulators and analogues for weed seed bank control.

In a previous study, Zwanenburg *et al.*[29] synthesised an active *N*-substituted phthalimide named Nijmegen-1 (Fig. 1). The structure of this compound is analogous to the typical ring structure of a strigolactone. The authors stated that a C ring was not necessary, but a D ring and an α,β-unsaturated carbonyl system were essential for activity. Furthermore, the aromatic ring could be modified without the risk of a reduction in activity.

A later study on branching inhibition[30] included simpler structures with activity and led to the idea that such structures could be used to stimulate seed germination. Several compounds with moderate activity have been proposed that lack the enol ether unit, and these were called strigolactone mimics, such as the

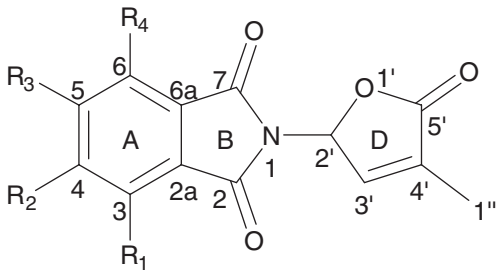

Figure 2. Numbered structure of phthalimide-lactone.

SL-mimic in Fig. 1,[31] which differ from strigolactone analogues on the assumption that their mode of action is also different.

The inclusion of a butenolide fragment can enhance pre-existing activity. In a previous study[32] we introduced the butenolide as a D ring in dehydrocostuslactone to obtain a strigolactone analogue. Dehydrocostuslactone is exuded by sunflower[7] and is a specific germination factor of *O. cumana*. The resulting compound, which is named guaianestrigolactone (Fig. 1), had enhanced activity in stimulating the germination of both *P. ramosa* and *O. cumana*.

The objective of the work described here was to assess a collection of *N*-substituted phthalimides for their ability to induce suicidal germination. The criteria for the selection of target molecules were the availability of the starting materials, the presence of different functional groups in the aromatic ring, and the molecular size. We present strigolactone mimics in which the D ring is bonded to the phthalimide and one α,β-unsaturated system has been removed, thus simplifying the system and the synthesis (Figs 2 and 3).

Four of the most economically important broomrape weeds were tested, namely *O. cumana*, *O. minor*, *P. aegyptiaca* and *P. ramosa*. These species span the broomrape spectrum in terms of taxonomic genera and the sensitivity of crop recognition at the levels of whole root exudate and chemical class of germination stimulants to which they are mainly sensitive.

2 EXPERIMENTAL METHODS

2.1 General experimental procedures

The purities of the compounds were determined by ^{1}H NMR spectroscopy. ^{1}H NMR and ^{13}C NMR spectra were recorded using $CDCl_3$ and acetone-d_6 (MagniSolv™; Merck) as solvents on Agilent™ 400 and 500 MHz spectrometers. The residual peaks were used as

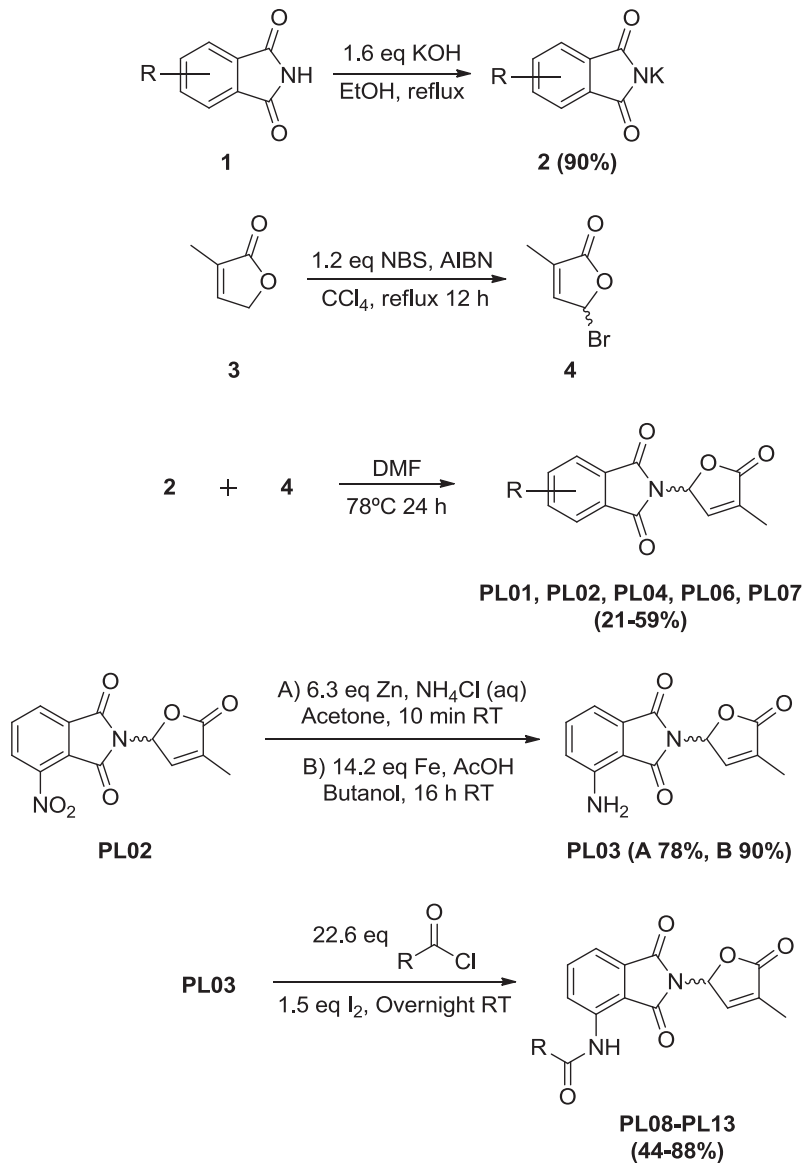

Figure 3. Synthesis of phthalimide-lactones.

the internal reference. Compounds **PL01** to **PL03** and compounds **PL06** to **PL13** were dissolved in $CDCl_3$, and the resonance of the residual chloroform was set to δ 7.26 ppm in ^{1}H NMR and to δ 77.0 ppm in ^{13}C NMR. Compounds **PL04** and **PL05** and compounds **PL14** to **PL19** were dissolved in acetone-d_6, and the residual acetone signal was set to δ 2.04 ppm in ^{1}H NMR and to δ 29.9 ppm in ^{13}C NMR. Mass spectra were recorded on a Thermo QExactive™ spectrometer equipped with an ESI source in positive mode with a resolution of 70 000 and an ionisation potential of 3500 V. UV–vis spectra were obtained using a Varian Cary 50 BIO spectrophotometer with methanol as the solvent. FTIR spectra were obtained on a Perkin-Elmer Spectrum Two IR spectrophotometer. Frequency values are given as wave numbers $\tilde{\nu}$ in cm^{-1}.

2.2 Preparation of derivatives

The starting materials were supplied by Alfa Aesar (Ward Hill, MA). *N*-Bromosuccinimide (NBS), 3-methyl-2(5*H*)-furanone (technical grade, 90%) and acyl chlorides were supplied by Sigma-Aldrich Co. (St Louis, MO). α,α'-Azobisisobutyronitrile (AIBN) was supplied by Merck (Darmstadt, Germany). Silica gel Geduran® Si 60 (0.063–0.200 mm) was used for column chromatography.

2.2.1 *General procedure for phthalimide salt preparation (**2**)*

Phthalimide **1** (1 g) was dissolved in 40 mL of ethanol at reflux with stirring. When dissolution was complete, a solution of 716 mg of KOH (11 mmol) in 10 mL of ethanol was added in several portions. The salt precipitated and the reaction mixture was stirred until further precipitation was not observed. The mixture was cooled in an ice bath and the precipitate was filtered off and washed with ethanol to give an approximate yield of 90% in all cases.

2.2.2 *5-Bromo-3-methyl-2(5H)-furanone (**4**)*

Freshly crystallised NBS (438 mg, 2.46 mmol) was added to 5 mL of CCl_4 and the mixture was heated under reflux with stirring for several minutes to promote NBS dissolution. Quantities of 200 μL of furanone **3** (2.05 mmol) and 3 mg of AIBN (0.02 mmol) were added, and the mixture was heated under reflux for 12 h. The

mixture was cooled to 0 °C and the solid NBS was filtered off. CCl_4 was evaporated under reduced pressure to afford a yellowish oil. The brominated products are unstable and further purification was not carried out prior to the next reaction.

2.2.3 Preparation of phthalimide-lactones (*PL*)

4-Nitrophthalimide salt **2** (300 mg, 1.30 mmol) was added to a solution of compound **4** (240 mg, 1.30 mmol) in 1 mL of dry DMF, and the mixture was heated at 78 °C with stirring for 24 h. The product *N*-(4-methyl-5-oxo-2,5-dihydrofuran-2-yl)-4-nitrophthalimide (**PL04**) was purified by column chromatography using a mixture of hexane: acetone (4: 1) as eluent. Similar procedures were used for compounds **PL01**, **PL02**, **PL06** and **PL07**.

2.2.4 Preparation of amino-phthalimide-lactones (*PL03*, *PL05*)

Two different procedures were employed to reduce the nitro group: (a) Zn (powder) and (b) Fe (powder).[33]

(a) *N*-(4-Methyl-5-oxo-2,5-dihydrofuran-2-yl)-3-nitrophthalimide **PL02** (35 mg, 0.121 mmol) was dissolved in acetone (2 mL) with sonication. Quantities of 50 mg of powdered Zn (0.765 mmol) and 0.37 mL of aqueous NH_4Cl (90 g mL^{-1}) were added to the solution. The mixture was sonicated for 10 min and the starting material was completely consumed (TLC). The mixture was filtered through Celite and the pad was washed with acetone and water. The acetone was evaporated under reduced pressure and the resulting aqueous product was extracted with ethyl acetate (×3). The organic layers were combined and dried over anhydrous $MgSO_4$, and the solvent was evaporated. **PL03** was isolated by column chromatography using a mixture of hexane: acetone (3: 2) as eluent. The same procedure was followed with *N*-(4-methyl-5-oxo-2,5-dihydrofuran-2-yl)-4-nitrophthalimide, **PL04**, to obtain **PL05**.

(b) *N*-(4-Methyl-5-oxo-2,5-dihydrofuran-2-yl)-3-nitrophthalimide **PL02** (33 mg, 0.115 mmol) was dissolved in 12 mL of butanol at 60 °C. Quantities of 91 mg of powdered iron (1.63 mmol) and 3.4 mL of acetic acid (59.4 mmol) were added. The reaction mixture was stirred for 16 h. The mixture was filtered through Celite, and 100 mL of ethyl acetate and 100 mL of deionised water were added. The organic layer was washed 3 times with deionised water and twice with saturated aqueous $NaHCO_3$. The organic layer was dried over anhydrous $MgSO_4$ and the solvent was evaporated. Isolation was carried out as described above. The same procedure was followed with **PL04** to obtain **PL05**.

2.2.5 Preparation of carbamoyl-phthalimide-lactones (*PL08 to PL19*)[34]

N-(4-Methyl-5-oxo-2,5-dihydrofuran-2-yl)-3-aminophthalimide **PL03** (40 mg, 0.155 mmol) was added to 250 μL of acetyl chloride (3.5 mmol). The mixture was stirred until complete dissolution, and 59 mg of iodine (0.233 mmol) was added. The mixture was stirred overnight. The reaction was quenched with 10 mL of saturated aqueous $Na_2S_2O_7$. Quantities of 40 mL of $Na_2S_2O_7$ and 50 mL of ethyl acetate were added. The aqueous layer was extracted with ethyl acetate (×3). The combined organic extracts were washed with 100 mL of saturated aqueous $NaHCO_3$ (×5) and dried over anhydrous $MgSO_4$, and the solvent was evaporated under reduced pressure. **PL08** was purified by column chromatography using a mixture of hexane: acetone (4: 1). The same procedure was followed with **PL03** to obtain **PL09** to **PL13** and with *N*-(4-methyl-5-oxo-2,5-dihydrofuran-2-yl)-4-aminophthalimide, **PL05**, to obtain **PL14** to **PL19**.

The structures of 19 *N*-substituted racemic phthalimides (Fig. 4) were confirmed by spectroscopic analysis: ^{1}H NMR, ^{13}C NMR, MS, FTIR and UV–vis.

N-*(4-Methyl-5-oxo-2,5-dihydrofuran-2-yl)phthalimide (**PL01**)*. A white solid was obtained in 43% yield from **2**, mp 162–163 °C. Spectroscopic data: HRMS, *m/z* (M^+) calcd for $C_{13}H_9O_4NNa$ 266.0424, found 266.0417; IR $\tilde{\nu}_{max}$ 3095, 2922, 1783, 1768, 1722, 1389, 1366 cm^{-1}; UV λ_{max} (MeOH) 273 nm (ε 5900), 219 nm (ε 5000). The ^{1}H NMR and ^{13}C NMR data are shown in Tables 1 and 2 respectively.

N-*(4-Methyl-5-oxo-2,5-dihydrofuran-2-yl)-3-nitrophthalimide (**PL02**)*. A white solid was obtained in 54% yield from **2**, mp 158–159 °C. Spectroscopic data: HRMS, *m/z* (M^+) calcd for $C_{13}H_8O_6N_2Na$ 311.0275, found 311.0268; IR $\tilde{\nu}_{max}$ 3098, 2937, 1771, 1733, 1542, 1385, 1361, 1321 cm^{-1}; UV λ_{max} (MeOH) 216 nm (ε 26 450). The ^{1}H NMR and ^{13}C NMR data are shown in Tables 1 and 2 respectively.

N-*(4-Methyl-5-oxo-2,5-dihydrofuran-2-yl)-3-aminophthalimide (**PL03**)*. A yellow solid was obtained from **PL02** in 90% yield in the reduction with Fe and 78% with Zn, mp 192–193 °C. Spectroscopic data: HRMS, *m/z* (M^+) calcd for $C_{13}H_{10}O_4N_2Na$ 281.0533, found 281.0526; IR $\tilde{\nu}_{max}$ 3478, 3373, 2925, 1764, 1708, 1634, 1483, 1363 cm^{-1}; UV λ_{max} (MeOH) 393 nm (ε 4350), 260 nm (ε 8200), 237 nm (ε 14 100), 225 nm (ε 22 100). The ^{1}H NMR and ^{13}C NMR data are shown in Tables 1 and 2 respectively.

N-*(4-Methyl-5-oxo-2,5-dihydrofuran-2-yl)-4-nitrophthalimide (**PL04**)*. A white solid was obtained in 59% yield from **2**, mp 186–187 °C. Spectroscopic data: HRMS, *m/z* (M^+) calcd for $C_{13}H_8O_6N_2Na$ 311.0275, found 311.0266; IR $\tilde{\nu}_{max}$ 3106, 2927, 1771, 1732, 1540, 1345, 772 cm^{-1}; UV λ_{max} (MeOH) 233 nm (ε 39 303), 204 nm (ε 57 123). The ^{1}H NMR and ^{13}C NMR data are shown in Tables 1 and 2 respectively.

N-*(4-Methyl-5-oxo-2,5-dihydrofuran-2-yl)-4-aminophthalimide (**PL05**)*. A yellow solid was obtained from **PL04** in 59% yield in the reduction with Fe and 33% with Zn, mp 229–231 °C. Spectroscopic data: HRMS, *m/z* (M^+) calcd for $C_{13}H_{10}O_4N_2Na$ 281.0533, found 281.0526; IR $\tilde{\nu}_{max}$ 3471, 3371, 2918, 1765, 1714, 1613, 1505, 1362 cm^{-1}; UV λ_{max} (MeOH) 377 nm (ε 3465), 314 nm (ε 4554), 259 nm (ε 17 820), 211 nm (ε 19 404). The ^{1}H NMR and ^{13}C NMR data are shown in Tables 1 and 2 respectively.

N-*(4-Methyl-5-oxo-2,5-dihydrofuran-2-yl)-2,3-naphthalenedicarboximide (**PL06**)*. A white solid was obtained in 21% yield from **2**, mp 198–202 °C. Spectroscopic data: HRMS, *m/z* (M^+) calcd for $C_{17}H_{11}O_4NNa$ 316.0580, found 316.0574; IR $\tilde{\nu}_{max}$ 2926, 1771, 1725, 1715, 765 cm^{-1}; UV λ_{max} (MeOH) 359 nm (ε 4257), 293 nm (ε 7029), 260 nm (ε 63 756), 217 nm (ε 36 531). The ^{1}H NMR and ^{13}C NMR data are shown in Tables 1 and 2 respectively.

N-*(4-Methyl-5-oxo-2,5-dihydrofuran-2-yl)-4,5-dichlorophthalimide (**PL07**)*. A white solid was obtained in 53% yield from **2**, mp 193–197 °C. Spectroscopic data: HRMS, *m/z* (M^+) calcd for $C_{13}H_7O_4NCl_2Na$ 333.9644, found 333.9639; IR $\tilde{\nu}_{max}$ 3095, 2924, 1767, 1719, 1715, 1387, 1367, 808, 743 cm^{-1}; UV λ_{max} (MeOH) 283 nm (ε 1250), 234 nm (ε 35 550), 213 nm (ε 31 350). The ^{1}H NMR and ^{13}C NMR data are shown in Tables 1 and 2 respectively.

N-*(4-Methyl-5-oxo-2,5-dihydrofuran-2-yl)-3-acetylaminophthalimide (**PL08**)*. A white solid was obtained from **PL03** in 44% yield, mp 208–209 °C. Spectroscopic data: HRMS, *m/z* (M^+) calcd for $C_{15}H_{12}O_5N_2Na$ 323.0638, found 323.0632; IR $\tilde{\nu}_{max}$ 3363, 2925, 2853, 1774, 1714, 1618, 1528, 1479, 1393, 1369, 1346 cm^{-1}; UV λ_{max} (MeOH) 342 nm (ε 3350), 254 nm (ε 10 250), 228 (ε 34 850). The ^{1}H NMR and ^{13}C NMR data are shown in Tables 3 and 4 respectively.

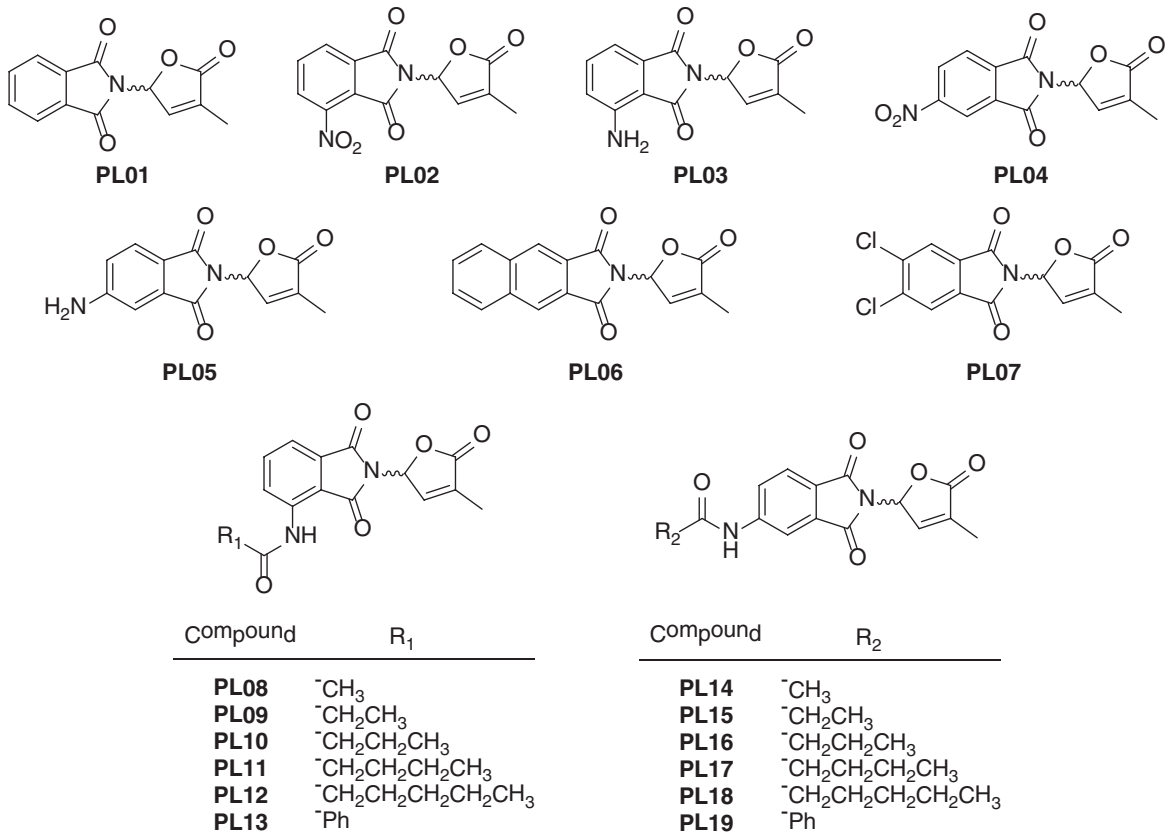

Figure 4. Structures of compounds **PL01** to **PL19**.

Table 1. ^{1}H NMR assignments for compounds **PL01** to **PL07**

Position	PL01 δ (J, Hz)	PL02 δ (J, Hz)	PL03 δ (J, Hz)	PL04 δ (J, Hz)	PL05 δ (J, Hz)	PL06 δ (J, Hz)	PL07 δ (J, Hz)
3	7.88, dd (5.5, 3)	–	–	8.61, dd (2, 0.6)	7.06, dd (2.1, 0.4)	8.39, s	7.97, s
4	7.80, dd (5.5, 3)	8.17, dd (7.5, 0.9)	6.89, dd (8.3, 0.6)	–	–	8.08, dd (6.2, 3.2)	–
5	7.80, dd (5.5, 3)	7.99, dd (7.9, 7.5)	7.46, dd (8.3, 7.2)	8.74, dd (8.2, 2)	6.99, dd (8.3, 2.1)	7.74, dd (6.2, 3.2)	–
6	7.88, dd (5.5, 3)	8.18, dd (7.9, 0.9)	7.17, dd (7.2, 0.6)	8.21, dd (8.2, 0.6)	7.55, dd (8.3, 0.4)	7.74, dd (6.2, 3.2)	7.97, s
7	–	–	–	–	–	8.08, dd (6.2, 3.2)	–
8	–	–	–	–	–	8.39, s	–
2′	6.67, m	6.67, dq (1.8, 1.9)	6.62, dq (1.8, 1.9)	6.75, dq (1.8, 1.9)	6.61, dq (1.8, 1.9)	6.75, dq (1.8, 1.9)	6.64, dq (1.8, 1.9)
3′	7.04, m	7.03, dq (1.8, 1.7)	7.03 dq (1.8, 1.7)	7.35, dq (1.8, 1.7)	7.31, dq (1.8, 1.7)	7.09, dq (1.8, 1.7)	7.01, dq (1.8, 1.7)
1″	2.06, m	2.06, dd (1.7, 1.9)	2.06, dd (1.7, 1.9)	1.98, dd (1.7, 1.9)	1.94, dd (1.7, 1.9)	2.09, dd (1.7, 1.9)	2.07, dd (1.7, 1.9)
NH	–	–	5.28, bs	–	6.1, bs	–	–

N-*(4-Methyl-5-oxo-2,5-dihydrofuran-2-yl)-3-propanoylamino-phthalimide (**PL09**)*. A white solid was obtained from **PL03** in 86% yield, mp 151–154 °C. Spectroscopic data: HRMS, *m/z* (M^+) calcd for $C_{16}H_{14}O_5N_2Na$ 337.0795, found 337.0787; IR $\tilde{\nu}_{max}$ 3361, 2924, 2852, 1775, 1714, 1618, 1528, 1480, 1393, 1367, 1346 cm^{-1}; UV λ_{max} (MeOH) 344 nm (ε 3350), 254 nm (ε 10 700), 228 (ε 25 500). The ^{1}H NMR and ^{13}C NMR data are shown in Tables 3 and 4 respectively.

N-*(4-Methyl-5-oxo-2,5-dihydrofuran-2-yl)-3-butanoylamino-phthalimide (**PL10**)*. A white solid was obtained from **PL03** in 88% yield, mp 117–122 °C. Spectroscopic data: HRMS, *m/z* (M^+) calcd for $C_{17}H_{16}O_5N_2Na$ 351.0951, found 351.0943; IR $\tilde{\nu}_{max}$ 3361, 2964, 2930, 2876, 1775, 1714, 1618, 1526, 1479, 1393, 1368, 1346 cm^{-1}; UV λ_{max} (MeOH) 344 nm (ε 5300), 255 nm (ε 17300), 228 (ε 41 100). The ^{1}H NMR and ^{13}C NMR data are shown in Tables 3 and 4 respectively.

N-*(4-Methyl-5-oxo-2,5-dihydrofuran-2-yl)-3-pentanoylamino-phthalimide (**PL11**)*. A white solid was obtained from **PL03** in 58% yield, mp 127–129 °C. Spectroscopic data: HRMS, *m/z* (M^+) calcd for $C_{18}H_{18}O_5N_2Na$ 365.1108, found 365.1103; IR $\tilde{\nu}_{max}$ 3360, 2958, 2929, 2872, 1775, 1715, 1618, 1526, 1479, 1393, 1368, 1345 cm^{-1}; UV λ_{max} (MeOH) 344 nm (ε 4300), 255 nm (ε 14 500), 228 (ε 34 850). The ^{1}H NMR and ^{13}C NMR data are shown in Tables 3 and 4 respectively.

N-*(4-Methyl-5-oxo-2,5-dihydrofuran-2-yl)-3-hexanoylamino-phthalimide (**PL12**)*. A white solid was obtained from **PL03** in 73% yield, mp 143–145 °C. Spectroscopic data: HRMS, *m/z* (M^+) calcd for $C_{19}H_{20}O_5N_2Na$ 379.1264, found 379.1259; IR $\tilde{\nu}_{max}$ 3361, 2957,

Table 2. ^{13}C NMR assignments for compounds **PL01** to **PL07**

Position	**PL01** δ	**PL02** δ	**PL03** δ	**PL04** δ	**PL05** δ	**PL06** δ^a	**PL07** δ
2	166.3	161.0	166.6	165.5	167.1	166.1	164.4
2a	131.4	–	145.9	–	156.3	126.8	130.4
3	134.8	123.2	110.5	119.5	108.3	125.8	126.0
3a	–	–	–	–	–	135.7	–
4	124.0	127.7	113.3	137.1	118.6	130.4	140.1
5	124.0	136.2	136.0	133.3	119.0	129.7	140.1
6	134.8	129.4	121.5	126.1	126.3	129.7	126.0
6a	131.4	134.1	133.3	137.1	135.4	–	130.4
7	166.3	163.9	168.1	165.7	167.7	130.4	164.4
7a	–	–	–	–	–	135.7	–
8	–	–	–	–	–	125.8	–
8a	–	–	–	–	–	126.8	–
9	–	–	–	–	–	166.1	–
2′	77.7	77.8	77.6	79.1	78.9	77.8	77.7
3′	141.9	141.2	142.2	144.1	144.9	142.0	141.3
4′	133.5	133.4	132.0	134.1	132.6	133.5	133.9
5′	171.7	171.3	171.9	172.5	172.8	171.8	171.4
1″	10.8	10.8	10.8	10.7	10.7	10.8	10.8

2929, 2872, 1776, 1715, 1618, 1527, 1479, 1393, 1367, 1346 cm^{-1}; UV λ_{max} (MeOH) 344 nm (ε 4400), 255 nm (ε 14 150), 228 (ε 32 250). The ^1H NMR and ^{13}C NMR data are shown in Tables 3 and 4 respectively.

N-*(4-Methyl-5-oxo-2,5-dihydrofuran-2-yl)-3-benzoylamino-phthalimide (**PL13**)*. A white solid was obtained from **PL03** in 58% yield, mp 138–142 °C. Spectroscopic data: HRMS, *m/z* (M^+) calcd for $C_{20}H_{14}O_5N_2Na$ 385.0795, found 385.0789; IR $\tilde{\nu}_{max}$ 3361, 3091, 3028, 2925, 2854, 1774, 1714, 1688, 1620, 1538, 1494, 1479, 1393, 1367, 1347 cm^{-1}; UV λ_{max} (MeOH) 344 nm (ε 4800), 269 nm (ε 17 850), 231 (ε 35 200). The ^1H NMR and ^{13}C NMR data are shown in Tables 3 and 4 respectively.

N-*(4-Methyl-5-oxo-2,5-dihydrofuran-2-yl)-4-acetylaminophthalimide (**PL14**)*. A white solid was obtained from **PL05** in 70% yield, mp 222–224 °C. Spectroscopic data: HRMS, *m/z* (M^+) calcd for $C_{15}H_{12}O_5N_2Na$ 323.0638, found 323.0631; IR $\tilde{\nu}_{max}$ 3333, 2924, 1777, 1723, 1615, 1548, 1491, 1435, 1364 cm^{-1}; UV λ_{max} (MeOH) 327 nm (ε 4950), 254 nm (ε 4500), 228 (ε 29 700). The ^1H NMR and ^{13}C NMR data are shown in Tables 3 and 4 respectively.

N-*(4-Methyl-5-oxo-2,5-dihydrofuran-2-yl)-4-propanoylamino-phthalimide (**PL15**)*. A white solid was obtained from **PL05** in 58% yield, mp 209–213 °C. Spectroscopic data: HRMS, *m/z* (M^+) calcd for $C_{16}H_{14}O_5N_2Na$ 337.0795, found 337.0788; IR $\tilde{\nu}_{max}$ 3335, 2925, 2853, 1775, 1777, 1723, 1614, 1546, 1491, 1435, 1361, 1323 cm^{-1}; UV λ_{max} (MeOH) 327 nm (ε 5050), 290 nm (ε 4800), 249 (ε 29 350). The ^1H NMR and ^{13}C NMR data are shown in Tables 3 and 4 respectively.

N-*(4-Methyl-5-oxo-2,5-dihydrofuran-2-yl)-4-butanoylamino-phthalimide (**PL16**)*. A white solid was obtained from **PL05** in 84% yield, mp 195–198 °C. Spectroscopic data: HRMS, *m/z* (M^+) calcd for $C_{17}H_{16}O_5N_2Na$ 351.0951, found 351.0947; IR $\tilde{\nu}_{max}$ 3348, 2963, 2928, 1777, 1723, 1679, 1614, 1543, 1492, 1434, 1361, 1324 cm^{-1}; UV λ_{max} (MeOH) 327 nm (ε 4800), 290 nm (ε 4450), 249 (ε 27 900), 210 (ε 23 800). The ^1H NMR and ^{13}C NMR data are shown in Tables 3 and 4 respectively.

N-*(4-Methyl-5-oxo-2,5-dihydrofuran-2-yl)-4-pentanoylamino-phthalimide (**PL17**)*. A white solid was obtained from **PL05** in 86% yield, mp 209–213 °C. Spectroscopic data: HRMS, *m/z* (M^+) calcd for $C_{18}H_{18}O_5N_2Na$ 365.1108, found 365.1106; IR $\tilde{\nu}_{max}$ 3330, 2958, 2927, 2872, 1778, 1724, 1614, 1544, 1491, 1434, 1360, 1323 cm^{-1}; UV λ_{max} (MeOH) 327 nm (ε 5100), 290 nm (ε 4950), 249 (ε 29 100), 207 (ε 26 200). The ^1H NMR and ^{13}C NMR data are shown in Tables 3 and 4 respectively.

N-*(4-Methyl-5-oxo-2,5-dihydrofuran-2-yl)-4-hexanoylamino-phthalimide (**PL18**)*. A white solid was obtained from **PL05** in 89% yield, mp 199–202 °C. Spectroscopic data: HRMS, *m/z* (M^+) calcd for $C_{19}H_{20}O_5N_2Na$ 379.1264, found 379.1257; IR $\tilde{\nu}_{max}$ 3327, 2956, 2926, 2855, 1779, 1724, 1614, 1546, 1492, 1434, 1361, 1323 cm^{-1}; UV λ_{max} (MeOH) 327 nm (ε 5550), 290 nm (ε 5350), 249 (ε 31 650), 207 (ε 29 050). The ^1H NMR and ^{13}C NMR data are shown in Tables 3 and 4 respectively.

N-*(4-Methyl-5-oxo-2,5-dihydrofuran-2-yl)-4-benzoylamino-phthalimide (**PL19**)*. A white solid was obtained from **PL05** in 58% yield, mp 246–250 °C. Spectroscopic data: HRMS, *m/z* (M^+) calcd for $C_{20}H_{14}O_5N_2Na$ 385.0795, found 385.0791; IR $\tilde{\nu}_{max}$ 3346, 3064, 2923, 2851, 1778, 1724, 1682, 1614, 1541, 1493, 1448, 1432, 1360, 1348, 1324 cm^{-1}; UV λ_{max} (MeOH) 327 nm (ε 6900), 293 nm (ε 7350), 258 (ε 24 000), 229 (ε 20 400). The ^1H NMR and ^{13}C NMR data are shown in Tables 3 and 4 respectively.

2.3 Broomrape germination bioassays

Seeds of four broomrape species, *Orobanche cumana*, *O. minor*, *Phelipanche ramosa* and *P. aegyptiaca*, were surface sterilised by immersion in 0.5% (w/v) NaOCl and 0.02% (v/v) Tween 20 with sonication for 2 min. The samples were rinsed thoroughly with sterile distilled water and dried in a laminar air flow cabinet. Approximately 100 seeds of each broomrape species were placed separately on 9 mm diameter glass fibre filter paper (GFFP) discs moistened with 50 μL of sterile distilled water and conditioned in a 10 cm sterile petri dish in the dark at 20 °C for 10 days. GFFP discs were transferred in a laminar flow cabinet onto sterile filter paper to remove excess water, and they were then transferred to a new 10 cm sterile petri dish. The test samples were dissolved in acetone and diluted with sterilised MQ water to a concentration range of 100–0.1 μM. The final concentration of acetone was adjusted to 1% (v/v). Discs containing conditioned seeds were treated with a

Table 3. ^{1}H NMR assignments for compounds **PL08** to **PL19**

Position	**PL08** δ (J, Hz)	**PL09** δ (J, Hz)	**PL10** δ (J, Hz)	**PL11** δ (J, Hz)	**PL12** δ (J, Hz)	**PL13** δ (J, Hz)	**PL14** δ (J, Hz)	**PL15** δ (J, Hz)	**PL16** δ (J, Hz)	**PL17** δ (J, Hz)	**PL18** δ (J, Hz)	**PL19** δ (J, Hz)
3	–	–	–	–	–	9, dd (8.5, 0.6)	8.31, dd (1.9, 0.6)	8.34, dd (1.9, 0.6)	8.34, dd (1.8, 0.6)	8.34, dd (1.9, 0.6)	8.34, dd (1.9, 0.6)	8.51, dd (1.8, 0.4)
4	8.82, dd (8.5, 0.8)	8.84, dd (8.5, 0.7)	8.82, dd (8.4, 0.7)	8.82, dd (8.5, 0.7)	8.83, dd (8.5, 0.7)	–	–	–	–	–	–	–
5	7.72, dd (8.5, 7.3)	7.7, dd (8.5, 7.4)	7.69, dd (8.4, 7.5)	7.69, dd (8.5, 7.3)	7.7, dd (8.5, 7.3)	7.77, dd (8.5, 7.4)	7.96, dd (8.2, 1.9)	7.99, dd (8.2, 1.9)	7.98, dd (8.2, 1.8)	7.99, dd (8.2, 1.9)	7.99, dd (8.2, 1.9)	8.28, dd (8.2, 1.8)
6	7.53, dd (7.3, 0.8)	7.52, dd (7.4, 0.7)	7.5, dd (7.5, 0.7)	7.5, dd (7.3, 0.7)	7.51, dd (7.3, 0.7)	7.57, dd (7.4, 0.6)	7.82, dd (8.2, 0.6)	7.82, dd (8.2, 0.6)	7.82, dd (8.2, 0.6)	7.82, dd (8.2, 0.6)	7.82, dd (8.2, 0.6)	7.90, dd (8.2, 0.4)
2′	6.62, dq (1.8, 1.9)	6.62, dq (1.8, 1.9)	6.6, dq (1.8, 1.9)	6.6, dq (1.8, 1.9)	6.61, dq (1.8, 1.9)	6.64, dq (1.8, 1.9)	6.66, dq (1.8, 1.9)	6.67, dq (1.8, 1.9)	6.67, dq (1.8, 1.9)	6.67, dq (1.8, 1.9)	6.67, dq (1.8, 1.9)	6.69, dq (1.8, 1.9)
3′	7.04, dq (1.8, 1.7)	7.03, dq (1.8, 1.7)	7.03 dq (1.8, 1.7)	7.03, dq (1.8, 1.7)	7.03, dq (1.8, 1.7)	7.05, dq (1.8, 1.7)	7.33, dq (1.8, 1.7)	7.34, dq (1.8, 1.7)	7.34 dq (1.8, 1.7)	7.33, p (1.8, 1.7)	7.33, dq (1.8, 1.7)	7.36, dq (1.8, 1.7)
1″	2.06, dd (1.9, 1.7)	2.06, dd (1.9, 1.7)	2.04, dd (1.9, 1.7)	2.05, dd (1.9, 1.7)	2.05, dd (1.9, 1.7)	2.08, dd (1.9, 1.7)	1.96, dd (1.9, 1.7)	1.96, dd (1.9, 1.7)	1.96, dd (1.9, 1.7)	1.96, dd (1.9, 1.7)	1.96, dd (1.9, 1.7)	1.98, dd (1.9, 1.7)
2‴	2.26, s	2.49, q (7.5)	2.42, t (7.4)	2.44, t (7.6)	2.44, t (7.6)	–	2.26, s	2.46, q (7.5)	2.41, t (7.3)	2.44, t (7.5)	2.43, t (7.5)	–
3‴	–	1.27, t (7.5)	1.76, tq (7.4, 7.4)	1.71, tt (7.6, 7.5)	1.73, tt (7.6, 7.4)	7.97, dt (1.2, 6.9)	–	1.15, t (7.5)	1.7, tq (7.3, 7.4)	1.67, tt (7.5, 7.5)	1.69, tt (7.5, 7.4)	8.04, dt (1.3, 8.4)
4‴	–	–	1, t (7.4)	1.4, tq (7.5, 7.4)	1.36, m	7.57, m	–	–	0.95, t (7.4)	1.37, tq (7.5, 7.4)	1.33, m	7.57, dt (7.4, 8.4)
5‴	–	–	–	0.94, t (7.4)	1.36, m	7.57, m	–	–	–	0.91, t (7.4)	1.28, m	7.62, tt (7.4, 1.3)
6‴	–	–	–	–	0.9, t (7.1)	7.57, m	–	–	–	–	0.88, t (7.1)	7.57, dt (7.4, 8.4)
7‴	–	–	–	–	–	7.97, dt (1.2, 6.9)	–	–	–	–	–	8.04, td (1.3, 8.4)
NH	9.37, bs	9.40, bs	9.37, bs	9.38, bs	9.38, bs	10.33, bs	9.78, bs	9.71, bs	9.71, bs	9.72, bs	9.73, bs	10.11, bs

Table 4. ^{13}C NMR assignments for compounds **PL08** to **PL19**

Position	PL08 δ	PL09 δ	PL10 δ	PL11 δ	PL12 δ	PL13 δ	PL14 δ	PL15 δ	PL16 δ	PL17 δ	PL18 δ	PL19 δ
2	168.3	168.3	168.3	168.3	168.3	168.6	167.1	167.1	167.0	167.1	167.1	167.1
2a	138.1	138.2	138.1	138.1	138.1	138.3	146.6	146.7	147.0	146.6	146.7	146.6
3	114.9	114.9	114.9	114.9	114.9	115.5	114.1	114.1	114.0	114.2	114.2	115.2
4	125.4	125.4	125.4	125.4	125.4	125.4	126.3	127.7	126.1	126.2	126.2	126.8
5	136.8	136.8	136.7	137.0	136.7	136.9	124.8	125.6	124.7	124.8	124.9	125.9
6	118.6	118.4	118.4	118.4	118.4	118.7	125.6	126.2	125.5	125.6	125.6	125.5
6a	130.8	130.8	130.7	130.7	130.7	130.8	134.2	134.2	134.1	134.2	134.2	134.1
7	165.6	165.7	165.6	165.6	165.7	168.6	166.8	166.8	166.7	166.8	166.8	166.8
2′	77.5	77.5	77.5	77.5	77.5	77.6	78.9	78.9	78.8	78.9	78.9	79.0
3′	141.6	141.6	141.7	141.7	141.7	141.7	144.7	144.6	144.5	144.6	144.6	144.6
4′	133.7	133.7	133.6	133.6	133.6	133.7	132.9	132.9	132.8	132.9	132.9	132.9
5′	171.5	171.6	171.5	171.6	171.5	171.6	172.6	172.6	172.5	172.6	172.6	172.6
1″	10.8	10.8	10.7	10.7	10.7	10.8	10.7	10.7	10.6	10.7	10.7	10.7
1‴	169.2	173.0	172.2	172.4	172.5	165.6	169.9	173.7	172.8	173.0	173.0	167.0
2‴	24.9	31.0	39.8	37.6	37.9	133.1	24.5	30.9	39.6	37.6	37.8	135.4
3‴	–	9.2	18.6	27.2	24.8	127.3	–	9.6	19.3	28.1	25.7	128.6
4‴	–	–	13.6	22.2	31.2	129.0	–	–	13.9	23.0	32.2	129.5
5‴	–	–	–	13.7	22.3	132.8	–	–	–	14.2	23.2	133.1
6‴	–	–	–	–	13.8	129.0	–	–	–	–	14.3	129.5
7‴	–	–	–	–	–	127.3	–	–	–	–	–	128.6

50 μL aliquot of the respective test solution. Each treatment was replicated 3 times. Seeds treated with MQ water (containing 1% acetone) or the synthetic strigolactone **GR24** at a concentration of 100–0.1 μM were included as controls. The seeds were incubated in the dark at 20 °C for 7 days prior to examination for germination. Seeds with an emerged radicle through the seed coat were scored as germinated, as observed using a stereoscopic microscope at 30× magnification, and the percentage of germination was established for each dish.

2.4 Statistical analysis

Germination bioassays were performed twice with at least three replicates. Percentage data were approximated to a normal frequency distribution by means of angular transformation {180/π × arcsin[sqrt(%/100)]} and subjected to analysis of variance (ANOVA) using SPSS software for Windows, v. 21.0 (SPSS Inc., Chicago, IL). The significance of mean differences between each treatment against negative control was evaluated by the two-sided Dunnett's test. Null hypothesis was rejected at the level of 0.05.

2.5 Calculation of EC_{50} and log *P*

The bioactivity data were fitted to a sigmoidal dose–response model (constant slope) by employing the GraphPad Prism v.5.00 software package (GraphPad Software Inc.).[35] The mlog *P* values were estimated using the OSIRIS property explorer (ChemExper Inc.).[36] This software uses the Chou and Jurs algorithm, which is based on computed atom contributions.[37]

3 RESULTS AND DISCUSSION

3.1 Synthesis

Phthalimide salts were prepared using solutions of KOH in ethanol. A large excess of base was required to guarantee complete ionisation of the phthalimide. A strong base, i.e. KOH, was needed to remove the proton from the secondary amide. The precipitate was washed several times with ethanol in order to remove non-ionised phthalimide.

Bromination was carried out in CCl_4 with AIBN and NBS that had been freshly crystallised. AIBN was employed because the use of benzoyl peroxide as the radical initiator led to lower yields. The use of NBS that had not been recrystallised led to a significant increase in secondary products and lower yields in the subsequent step. It was important to remove traces of remaining NBS after the bromination by precipitation at 0 °C and subsequent filtration, as residual NBS could compete with the phthalimide salt in the nucleophilic substitution of the brominated lactone. The ^1H NMR spectrum of the filtered reaction mixture showed that NBS had been almost totally removed, and the peak area ratios for brominated/non-brominated lactones were higher than 9: 1. The ^1H NMR spectrum of the reaction mixture after 24 h showed that the starting material had been completely consumed, whereas after only 12 h this was not the case.

The yields obtained in the reduction of compounds **PL01** and **PL03** were higher on using Fe/acetic acid than with Zn/NH_4Cl, although in both cases Zn/NH_4Cl did produce the desired products. The low solubility of these compounds in a range of alcohols led us to use a large volume of butanol for the reduction with Fe, and long reaction times were also required. The synthesis of amides **PL08** to **PL19** led to varying results. In some cases, especially for the shortest chain lengths, the yields were particularly low (44%), but in other cases high yields were obtained (90%). It was found that an increase in the amount of acyl chloride and longer reaction times led to an increase in the yield. Thus, the yields obtained in the synthesis of **PL15** and **PL18** were improved from the initial 15 and 17% to 58 and 89% respectively.

3.2 General bioactivity profiles

The effects of structural modifications in the *N*-substituted phthalimides and the concentrations tested (range 100–0.1 μM) on conditioned seeds of broomrape species belonging to the

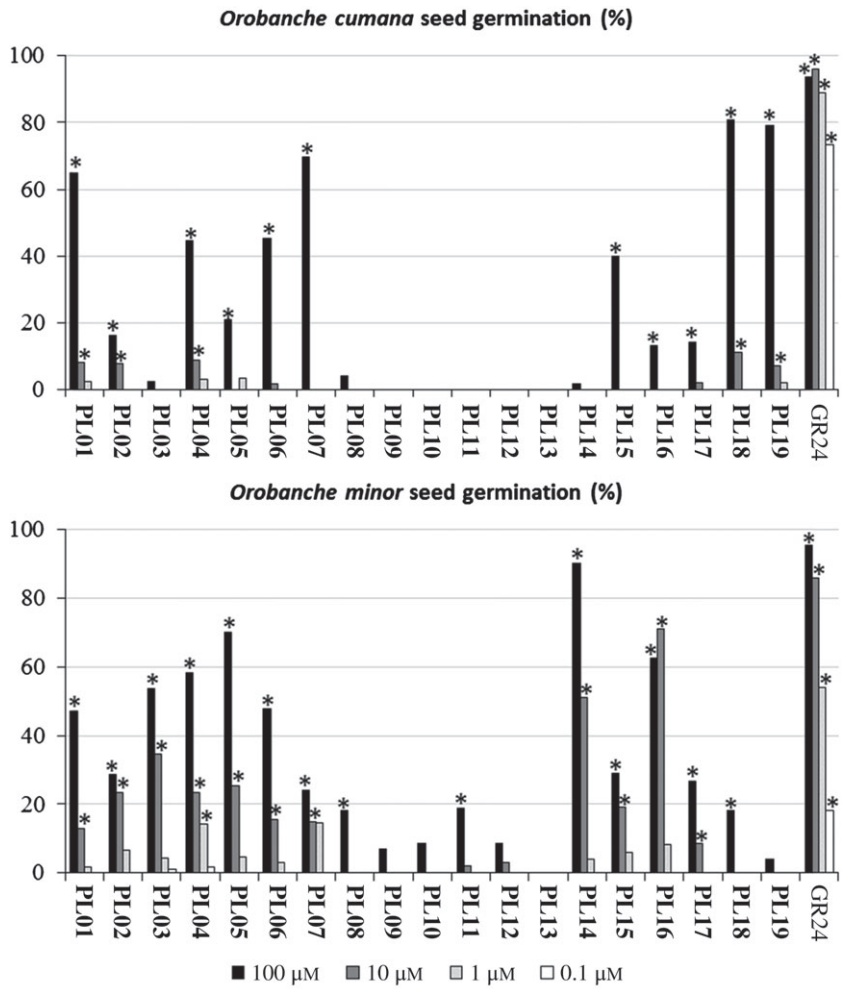

Figure 5. *Orobanche cumana* and *O. minor* seed germination induced by phthalimide-lactones. For each concentration, * indicates differences of each metabolite compared with the negative control (water) assesed by Dunnett's test at the 0.05 level.

genera *Orobanche* (*O. cumana* and *O. minor*) and *Phelipanche* (*P. aegyptiaca* and *P. ramosa*) are represented in Figs 5 and 6 respectively. In all cases, zero germination was observed when broomrape seeds were treated with the negative control (1% acetone in distilled water). Significant effects were observed for the phthalimides tested in the germination of *Orobanche* and *Phelipanche* (ANOVA, $P < 0.001$ in both cases), and germination was significantly affected by the phthalimide concentration (ANOVA, $P < 0.001$ in both cases). Concentration was positively related to the broomrape germination rate for all of the phthalimides tested. Interactions between the compound tested × broomrape species, concentration tested × broomrape species and compound tested × concentration tested were found to be significant (ANOVA, $P < 0.001$ in all cases).

The levels of *O. minor* and *O. cumana* seed germination induced by the *N*-substituted phthalimides were much lower than those observed for *Phelipanche* species. **PL14** and **PL16** induced the highest germination rates in *O. minor*, followed by **PL01**, **PL02**, **PL03**, **PL04**, **PL05**, **PL06**, **PL15** and **PL17**. The rest of the phthalimides induced very low or zero *O. minor* germination. The capacity for germination of these seeds was demonstrated by the germination values promoted by the positive control **GR24** (Fig. 5). Low or zero *O. cumana* seed germination was observed for the *N*-substituted phthalimide collection, except for **PL01**, **PL04**, **PL06**, **PL07**, **PL15**, **PL18** and **PL19** tested at 100 μM (Fig. 5).

P. aegyptiaca was the most sensitive broomrape species to phthalimide lactones, and all of the *N*-substituted phthalimides induced significant germination rates on seeds of *P. aegyptiaca* at 100 μM. The activity levels of **PL01**, **PL04**, **PL06**, **PL07** and **PL08** remained high on *P. aegyptiaca* seeds at lower concentrations. Previous studies have identified *P. aegyptiaca* as one of the broomrape species with the broadest recognition spectra for germination-inducing factors.[14,15]

PL01, **PL03**, **PL04**, **PL07**, **PL08**, **PL09**, **PL10** and **PL13** displayed the strongest activity on *P. ramosa* germination, while the phthalimides that caused the lowest induction of this species were **PL05**, **PL14**, **PL16**, **PL17**, **PL18** and **PL19**.

3.3 Analysis of EC_{50} and log *P*

EC_{50} and mlog *P* values are shown in Table 5. The calculated mlog *P* values are in the range 1–3 for all compounds, including **GR24**. These results are consistent with Lipinski's rule for bioactive compounds.[38] However, for each species, neither **PL08–PL13** nor **PL14–PL19** fitted a parabolic curve, so a clear relationship between EC_{50} and log *P* could not be established. Thus, the activity is not conditioned to transport phenomena and it must be linked to other electronic and steric interactions at the site

Table 5. EC_{50} values and calculated mlog *P* values (n.a. = not active)

	O. cumana		*O. minor*		*P. aegyptiaca*		*P. ramosa*		
	EC_{50} (μM)	R^2	EC_{50} (μM)	R^2	EC_{50} (μM)	R^2	EC_{50} (μM)	R^2	mlog *P*
GR24	0.0317	0.9948	0.816	0.9936	0.00214	0.9990	0.0129	0.9920	2.39
PL01	60.7	0.9957	109	0.9980	1.72	0.9933	11.9	0.9959	1.91
PL02	536	0.9964	275	0.9915	6.31	0.9998	58.7	0.9998	2.00
PL03	4383	1.000	61.6	0.9490	5.77	0.9984	11.9	0.9874	1.92
PL04	126	0.995	68.5	0.9811	1.35	0.9923	36.1	0.9976	2.00
PL05	391	0.9981	35.9	0.9975	13.7	0.9948	251	0.9938	1.41
PL06	123	0.9968	106	0.9951	1.78	0.9901	31.5	0.9984	2.77
PL07	58.4	0.9786	399	0.9737	2.52	0.9969	6.15	0.9795	2.97
PL08	2425	1.000	446	0.9996	3.09	0.9950	1.49	0.9802	1.50
PL09	n.a.	–	1287	0.9999	5.59	0.9952	7.45	0.9885	1.75
PL10	n.a.	–	1019	0.9999	6.01	0.9991	11.0	0.9831	1.99
PL11	n.a.	–	425	1.000	12.9	0.9990	78.5	0.9874	2.23
PL12	n.a.	–	1067	0.9996	44.2	0.9996	55.3	0.9964	2.46
PL13	n.a.	–	n.a.	–	11.7	0.9998	6.68	0.9421	2.73
PL14	6073	1.000	9.69	0.9981	47.5	0.9996	494	0.9998	1.50
PL15	152	0.9965	262	0.9765	11.8	0.9911	199	0.9987	1.75
PL16	647	0.9998	3.77	0.9188	20.3	0.9911	418	0.9960	1.99
PL17	605	1.000	277	0.9971	56.3	0.9988	634	0.9990	2.23
PL18	38.3	0.9869	446	0.9996	77.0	0.9957	618	0.9891	2.46
PL19	42.8	0.9814	2302	1.000	154	0.9969	545	0.9997	2.73

of action. Nevertheless, some trends were apparent from these results.

PL01, **PL07**, **PL18** and **PL19** have the best EC_{50} values for *O. cumana*, with mlog $P \geq 1.91$. The highest activity was found for **PL18**, with mlog $P = 2.46$, i.e. very similar to that of the reference **GR24** (mlog *P* 2.39). The compounds with the lowest mlog *P* values were **PL05**, **PL08** and **PL14** (mlog *P* 1.41, 1.50, 1.50 respectively). Of these compounds, **PL14** (EC_{50} 6073 μM) was the least active, although the activity of **PL03** was of the same order of magnitude (EC_{50} 4383 μM, mlog *P* 1.92). In conclusion, for good activity, the mlog *P* value should be ≥1.9, but other interactions must also be considered.

PL05, **PL14** and **PL16** were the most active on *O. minor* (mlog *P* 1.41, 1.50 and 1.75 respectively), and these compounds all had mlog $P < 2$. **PL09**, **PL10**, **PL12** and **PL19** were the least active compounds in this case. Of these compounds, **PL19** had the highest mlog *P* (2.73), but the activity of **PL09** was of the same order of magnitude, despite it having a lower mlog *P* (1.75). The volume of the molecule may be an important factor for activity; **PL19** has an amide at C-4 with an aromatic ring and **PL09** has an amide at C-3 with a propanoyl chain. In conclusion, a value of mlog $P \leq 2.00$ is preferred, but once again other interactions may contribute significantly to the activity.

A clear trend was observed on *P. aegyptiaca* in that **PL08** and **PL15** were the most active amides. These compounds have substituents at C-3 and C-4 respectively. The activity in each group decreased with mlog *P*, although there were some exceptions. **PL13** has the highest mlog *P* in group C-3 and it was more active than **PL12**, whereas **PL14** has the lowest mlog *P* of the compounds with a substituent at C-4 and was less active than **PL15**. Similar behaviour was observed for the other compounds in the series. For example, **PL07** has the highest mlog *P* and also has one of the lowest EC_{50} values (2.97, 2.52 μM), but **PL06**, with a lower mlog *P*, has a lower EC_{50} (2.77, 1.78 μM). Once again it is apparent that consideration of the transport phenomena alone is not sufficient to explain the results.

In general, the EC_{50} values were higher on *P. ramosa* than on *P. aegyptiaca*. Amides **PL08** to **PL13** showed two trends. Compounds **PL08** to **PL10** showed a decrease in EC_{50} with mlog *P*, whereas EC_{50} increased with mlog *P* for **PL11** to **PL13**. A clear trend with mlog *P* was not observed for the other amides and the remaining compounds, and this parameter alone is therefore not responsible for the observed bioactivity.

3.4 Structure–activity relationships

It can be seen from the results in Table 5 that the compounds were not equally effective on all of the species based on the EC_{50} value. In particular, for *Phelipanche* spp., substitution at position 3 (**PL08** to **PL13**) was preferred over position 4 (**PL14** to **PL19**), and for *Orobanche* spp. the opposite trend was found. This behaviour was found in both nitro- and amino-derivatives (**PL02** to **PL05**), with the exception of compound **PL04** on *Phelipanche*, for which the EC_{50} was lower than that of **PL02**. Furthermore, compounds **PL01**, **PL04**, **PL06** and **PL07** showed good EC_{50} values for all the species tested.

O. cumana was selectively stimulated by amides at C-4 and long chain lengths were preferred (**PL18** and **PL19**). Amines (**PL03** and **PL05**) were less active than the corresponding nitro compounds (**PL02** and **PL04**). High EC_{50} values for **PL02**, **PL03** and amides **PL08** to **PL13** showed that substitution at C-3 had a negative effect on activity. **PL01**, which has an unsubstituted aromatic ring, had a low EC_{50} value. The effect of substitution at C-4 and C-5 can be seen for **PL06**, with the inclusion of an additional aromatic ring, and **PL07**, with a chlorinated aromatic ring, when compared with **PL01**. **PL07** had similar activity to **PL01**, but the activity of **PL06** was lower. In any case, this decrease was only slight compared with the changes observed for other compounds, and the associated mlog *P*, a factor that has a marked effect on solubility, was much higher in both **PL06** and **PL07**.

O. minor was less selective to **PL** stimulation and substitution at C-3 had a greater effect (**PL08** to **PL13**). Of the compounds

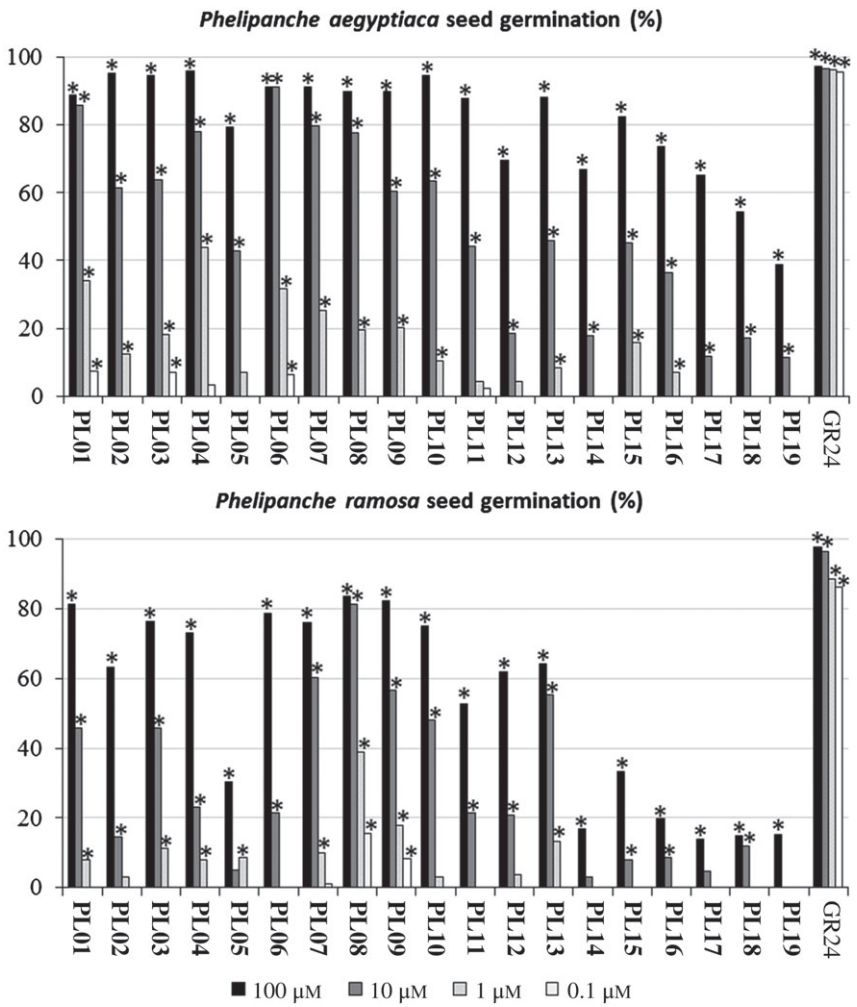

Figure 6. *Phelipanche aegyptiaca* and *P. ramosa* seed germination induced by phthalimide-lactones. For each concentration, * indicates differences of each metabolite compared with the negative control (water) assesed by Dunnett's test at the 0.05 level.

with amide groups at C-4 (**PL14** to **PL19**), **PL16** had the highest activity, followed by **PL14**. The medium and shorter chain lengths seem to be preferred in this case, which is in contrast to the trend for *O. cumana*. Selectivity was also found for amino (**PL03** and **PL05**) versus nitro (**PL02** and **PL04**) groups – also in contrast to the behaviour observed for *O. cumana*. Comparison of **PL01** with **PL07** showed that chlorination at C-4 and C-5 had a negative effect on activity. The inclusion of an additional aromatic ring in **PL06** did not have a significant effect on activity, but it did lead to a higher mlog *P*.

In general, *Phelipanche* spp. were less structure specific than *Orobanche* spp., and *P. aegyptiaca* were more sensitive to **PL** stimulation than *P. ramosa*. In the case of *P. aegyptiaca*, substitution at C-3 was better in terms of EC_{50}, but the results for compounds with a C-4 substituent are still remarkable. In contrast, *P. ramosa* showed more specificity for C-3-substituted compounds, with far lower EC_{50} values than the C-4-substituted compounds. Both *Phelipanche* spp. were stimulated more by the amine **PL03** than the nitro compound **PL02**.

PL04, which contains a nitro group at C-4, was the most active compound on *P. aegyptiaca*, followed by **PL01**, **PL06** and **PL07**. Substitution at C-4 led to a decrease in activity for the amides (**PL14** to **PL19**), but it did not have a significant effect on the most active compounds. In fact, the presence of a nitro group at C-4 led to a slightly higher activity than for **PL01**. Further research is required to explain this behaviour.

Finally, on *P. ramosa* the most active compounds were those with an amide at C-3 (**PL08** to **PL13**), followed by the compound with an amino group at C-3 (**PL03**), which showed the same activity as **PL01**.

A preliminary hypothesis is that the substituent on the aromatic ring could play an important role in the selectivity of these species. For example, the unsubstituted compound **PL01** is active on all of the species tested, but the presence of substituents at C-3 and C-4 had a marked effect on the activity. The volume of the molecule seems to play a key role, but the lack of a correlation between the EC_{50}, mlog *P* and chain size precluded any firm conclusions on this matter.

In general, the different responses to **PL** could indicate that the least specific species, *P. aegyptiaca*, is adapted to different types of molecules exuded by the hosts. Thus, the stimulation is similar upon exposure to different structures. The opposite behaviour was observed when the more specific *O. cumana* was exposed to different structures. The results offer clues to the structural requirements for the design of specific or multitarget stimulants. However, a larger collection of compounds with substituents in other positions and other functional groups is required to clarify this matter.

In summary, **PL01**, **PL06** and **PL07** can be selected for the stimulation of different species of *Orobanche* and *Phelipanche*, but specificity towards a genus or a species can be achieved by modifying the chain length or the substitution pattern in the aromatic ring. It was found that compounds with a substituent at C-3 are preferred for *Phelipanche* germination, and those at C-4 for *Orobanche*.

4 CONCLUSIONS

The synthesis of a diverse range of PLs was carried out in a few steps and with few changes to the experimental conditions to provide the target compounds in good yields. Further work is planned to select the most active examples as leads for new target compounds with different modifications in an effort to increase the activity and to design systems with the widest possible range of applications. Phthalimide derivatives have previously been described as germination inducers, but also as anti-inflamatory[39] and cytotoxic compounds.[40] Our ultimate aim is the design of easily synthesised and cheap multipurpose structures.

Studies into the stability of these compounds in soils, their bioavailability, cost and toxicological assays in animals and humans are required. The solubility of these materials in water is low, but it is high enough that they show activity. Further work will be carried out in order to evaluate their stability and to increase their solubility.

Synthetic phthalimides may constitute a cheap alternative for weed control,[27] and their potent effect in inducing broomrape germination suggests that this class of compounds is a good candidate for the promotion of bioregulator-induced suicidal germination of broomrape. These phthalimides can therefore aid the design of new ecofriendly broomrape-specific herbicides.

ACKNOWLEDGEMENTS

This research was supported by the Ministerio de Economía y Competitividad (MINECO), Spain, Project AGL2013-42238-R and COST Programme FA1206. M Fernández-Aparicio received support from the European Union, Marie-Curie FP7 COFUND People Programme, through the award of an AgreenSkills' fellowship (under Grant Agreement No. PCOFUND-GA-2010-267196), with additional support from INRA Division 'Santé des Plantes et Enviroment, appel à projets scientifiques 2015, Catégorie Biocontrôle'.

SUPPORTING INFORMATION

Supporting information may be found in the online version of this article.

REFERENCES

1 Parker C, Observations on the current status of *Orobanche* and *Striga* problems worldwide. *Pest Manag Sci* **65**:453–459 (2009).
2 Musselman L, The biology of *Striga*, *Orobanche*, and other root-parasitic weeds. *Annu Rev Phytopathol* **18**:463–489 (1980).
3 Lechat M-M, Brun G, Montiel G, Véronési C, Simier P, Thoiron S *et al.*, Seed response to strigolactone is controlled by abscisic acid-independent DNA methylation in the obligate root parasitic plant, *Phelipanche ramosa* L. Pomel. *J Exp Bot* **66**:3129–3140 (2015).
4 Lechat M-M, Pouvreau J-B, Péron T, Gauthier M, Montiel G, Véronési C *et al.*, PrCYP707A1, an ABA catabolic gene, is a key component of *Phelipanche ramosa* seed germination in response to the strigolactone analogue GR24. *J Exp Bot* **63**:5311–5322 (2012).
5 Zwanenburg B, Ćavar Zeljković S and Pospíšil T, Synthesis of strigolactones, a strategic account. *Pest Manag Sci* **72**:15–29 (2016).
6 Vurro M, Prandi C and Baroccio F, Strigolactones: how far is their commercial use for agricultural purposes? *Pest Manag Sci* DOI: 10.1002/ps.4254 (2016).
7 Joel DM, Chaudhuri SK, Plakhine D, Ziadna H and Steffens JC, Dehydrocostus lactone is exuded from sunflower roots and stimulates germination of the root parasite *Orobanche cumana*. *Phytochemistry* **72**:624–634 (2011).
8 Auger B and Pouvreau J, Germination stimulants of *Phelipanche ramosa* in the rhizosphere of *Brassica napus* are derived from the glucosinolate pathway. *Mol Plant–Microbe Interact* **25**:993–1004 (2012).
9 Evidente A, Fernández-Aparicio M, Cimmino A, Rubiales D, Andolfi A and Motta A, Peagol and peagoldione, two new strigolactone-like metabolites isolated from pea root exudates. *Tetrahedron Lett* **50**:6955–6958 (2009).
10 Evidente A, Cimmino A, Fernández-Aparicio M, Andolfi A, Rubiales D and Motta A, Polyphenols, including the new peapolyphenols A–C, from pea root exudates stimulate *Orobanche foetida* seed germination. *J Agric Food Chem* **58**:2902–2907 (2010).
11 Evidente A, Cimmino A, Fernandez-Aparicio M, Rubiales D, Andolfi A and Melck D, Soyasapogenol B and *trans*-22-dehydrocampesterol from common vetch (*Vicia sativa* L.) root exudates stimulate broomrape seed germination. *Pest Manag Sci* **67**:1015–1022 (2011).
12 Schneeweiss GM, Correlated evolution of life history and host range in the nonphotosynthetic parasitic flowering plants *Orobanche* and *Phelipanche* (Orobanchaceae). *J Evol Biol* **20**:471–478 (2007).
13 Parker C and Riches CR, *Parasitic Weeds of the World: Biology and Control*. CABI, Wallingford, Oxon, UK (1993).
14 Fernández-Aparicio M, Yoneyama K and Rubiales D, The role of strigolactones in host specificity of *Orobanche* and *Phelipanche* seed germination. *Seed Sci Res* **21**:55–61 (2011).
15 Fernández-Aparicio M, Flores F and Rubiales D, Recognition of root exudates by seeds of broomrape (*Orobanche* and *Phelipanche*) species. *Ann Bot* **103**:423–431 (2009).
16 Rubiales D, Fernández-Aparicio M, Wegmann K and Joel DM, Revisiting strategies for reducing the seedbank of *Orobanche* and *Phelipanche* spp. *Weed Res* **49**:23–33 (2009).
17 Zwanenburg B, *Mwakaboko AS and Kannan C*, Perspective of suicidal germination for parasitic weed control. Pest Manag Sci DOI: 10.1002/ps.4222 (2016).
18 Tasker AV and Westwood JH, The U.S. witchweed eradication effort turns 50: a retrospective and look-ahead on parasitic weed management. *Weed Sci* **60**:267–268 (2012).
19 Samejima H, Babiker AG, Takikawa H, *Sasaki M and Sugimoto Y*, Practicality of the suicidal germination approach for controlling *Striga hermonthica*. Pest Manag Sci DOI: 10.1002/ps.4215 (2016).
20 Lieberman M, Biosynthesis and action of ethylene. *Annu Rev Plant Physiol* **30**:533–591 (1979).
21 Logan DC and Stewart GR, Role of ethylene in the germination of the hemiparasite *Striga hermonthica*. *Plant Physiol* **97**:1435–1438 (1991).
22 Berner DK, Schaad NW and Völksch B, Use of ethylene-producing bacteria for stimulation of *Striga* spp. seed germination. *Biol Control* **15**:274–282 (1999).
23 Joel DM, The long-term approach to parasitic weeds control: manipulation of specific developmental mechanisms of the parasite. *Crop Prot* **19**:753–758 (2000).
24 Toh S, Kamiya Y, Kawakami N, Nambara E, McCourt P and Tsuchiya Y, Thermoinhibition uncovers a role for strigolactones in *Arabidopsis* seed germination. *Plant Cell Physiol* **53**:107–117 (2012).
25 Suttle JC and Schreiner DR, Effects of Dpx-4189 (2-chloro-*N*-((4-methoxy-6-methyl-1,3,5-triazin-2-Yl)aminocarbonyl)benzenesulfonamide) on anthocyanin synthesis, phenylalanine ammonia-lyase activity, and ethylene production in soybean hypocotyls. *Can J Bot* **60**:741–745 (1982).
26 Metzger JD, Promotion of germination of dormant weed seeds by substituted phthalimides and gibberellic-acid. *Weed Sci* **31**:285–289 (1983).
27 Villedieu-Percheron E, Zurwerra D, Lachia MD, De Mesmaeker A, Wolf HC, Jung PJM *et al.*, Plant growth regulating compounds. International Patent WO 2013/171092 A1 (2013).
28 Tsuchiya Y, Vidaurre D, Toh S, Hanada A, Nambara E, Kamiya Y *et al.*, A small-molecule screen identifies new functions for the plant hormone strigolactone. *Nat Chem Biol* **6**:741–749 (2010).
29 Nefkens GHL, Thuring JWJF, Beenakkers MFM and Zwanenburg B, Synthesis of a phthaloylglycine-derived strigol analogue and its

germination stimulatory activity toward seeds of the parasitic weeds *Striga hermonthica* and *Orobanche crenata*. *J Agric Food Chem* **45**:2273–2277 (1997).
30 Fukui K, Ito S, Ueno K, Yamaguchi S, Kyozuka J and Asami T, New branching inhibitors and their potential as strigolactone mimics in rice. *Bioorg Med Chem Lett* **21**:4905–4908 (2011).
31 Zwanenburg B and Pospísil T, Structure and activity of strigolactones: new plant hormones with a rich future. *Mol Plant* **6**:38–62 (2013).
32 Macías FA, García-Díaz MD, Pérez-de-Luque A, Rubiales D and Galindo JCG, New chemical clues for broomrape–sunflower host–parasite interactions: synthesis of guaianestrigolactones. *J Agric Food Chem* **57**:5853–5864 (2009).
33 Muceniece D, Popelis J and Lusis V, Substituent effect of 4- and 5-substituted 2-aryl-methylideneindane-1,3-diones on formation of 5-oxo-1*H*-4,5-dihydroindeno[1,2-*b*]pyridines. *Chem Heterocycl Compd* **44**:35–42 (2008).
34 Phukan K, Ganguly M and Devi N, Mild and useful method for *N*-acylation of amines. *Synth Commun* **39**:2694–2701 (2009).
35 *PRISM 5.00*. GraphPad Software, Inc., San Diego, CA (2007).
36 Sander T, *OSIRIS Property Explorer*. [Online]. Actelion Property Explorer (2001). Available: http://www.chemexper.com/tools/propertyExplorer/main.html [1 April 2015].
37 Chou J and Jurs P, Computer-assisted computation of partition coefficients from molecular structures using fragment constants. *J Chem Inf Comput Sci* **19**:172–178 (1979).
38 Lipinski CA, Lombardo F, Dominy BW and Feeney PJ, Experimental and computational approaches to estimate solubility and permeability in drug discovery and development settings. *Adv Drug Deliv Rev* **46**:3–26 (2001).
39 Lima LM, Castro P, Machado AL, Fraga CAM, Lugnier C, De Moraes VLG *et al.*, Synthesis and anti-inflammatory activity of phthalimide derivatives, designed as new thalidomide analogues. *Bioorg Med Chem* **10**:3067–3073 (2002).
40 Kok SHL, Gambari R, Chui CH, Yuen MCW, Lin E, Wong RSM *et al.*, Synthesis and anti-cancer activity of benzothiazole containing phthalimide on human carcinoma cell lines. *Bioorg Med Chem* **16**:3626–3631 (2008).

